Applied Catalysis B: Environmental 203 (2017) 314–323

Contents lists available at ScienceDirect

Applied Catalysis B: Environmental

journal homepage: www.elsevier.com/locate/apcatb

Efficient and ecofriendly route for the solvent-free synthesis of piperonal and aromatic aldehydes using Au/CeO_2 catalyst

C. Lucarelli[a,c,*], A. Lolli[b,c], A. Giugni[b], L. Grazia[b], S. Albonetti[b,c,*], D. Monticelli[a], A. Vaccari[b,c]

[a] Dipartimento di Scienza e Alta Tecnologia, University of Insubria, Via Valleggio 11, 22100, Como, Italy
[b] Dipartimento di Chimica Industriale "Toso Montanari", Alma Mater Studiorum, University of Bologna, Viale Risorgimento 4, 40136, Bologna, Italy
[c] Consorzio INSTM—UdR Bologna, Via G. Giusti, 9, 50121, Firenze, Italy

ARTICLE INFO

Article history:
Received 1 September 2016
Received in revised form 5 October 2016
Accepted 11 October 2016
Available online 13 October 2016

ABSTRACT

In this work, an eco-friendly process for piperonal synthesis from piperonyl alcohol oxidation was developed. Piperonal was obtained with 100% selectivity under solvent free conditions, using air as oxidant at atmospheric pressure. The preparation of high surface area CeO_2 using a surfactant-template method allowed the preparation of a catalyst with highly dispersed Au nanoparticles having an average diameter of about 1 nm. The obtained results, using Au/CeO_2 catalysts, suggested that the reaction network consists in the rapid oxidation of piperonyl alcohol to piperonal. Increasing reaction time to promote alcohol conversion a very small amount of formed aldehyde undergoes to further oxidation to the acid. Subsequently, piperonylic acid can easily react with the alcohol, leading to the formation of the ester that can be adsorbed on the catalyst surface, deactivating the materials. Nevertheless, the fine-tuning of the process, using solvent free conditions, air and low reaction time, demonstrated the possibility to control catalyst deactivation. Indeed, gold supported on nano-CeO_2 were able to catalyse the production of piperonal without by-product formation, with 35% of piperonyl alcohol conversion after 45 min of reaction and the catalyst can be recycled without any activity loss, demonstrating the possibility of scaling up a low conversion continuous process or low reaction time batch process.

No toxic reagents were used neither for catalysts preparation nor for catalytic tests and the use of air as oxidant improved the safety of the process. The latter, together with the absence of a solvent, can led to important advancements in the industrial applications reducing the costs of the purification section. This versatile approach, interesting from both the economic and the environmental point of view, was also applied in the synthesis of other aromatic aldehydes, such as benzaldehyde, vanillin and anysil aldehyde, highlighting the importance of this process.

© 2016 Elsevier B.V. All rights reserved.

1. Introduction

Piperonal [3,4-(methylenedioxy)benzaldehyde or heliotropin] is an important intermediate used in the synthesis of fragrances, cosmetic, pharmaceutical and agrochemical productions [1]. In general, it is industrially prepared by chromic acid oxidation [2] or isosafrole ozonolysis [3,4]. These processes have a strong environmental impact in terms of toxicity of the employed chemicals (Cr(VI) and ozone) and energy consumption for ozone production. The limited availability of safrole, isolated from the essential oil of *Ocotea Cymbarum* and *Pretiosa* trees, calls for the identification of alternative synthetic routes. The preparation of piperonal starting from 1,2-methylendioxybenzene or 3,4-dihydroxybenzaldehyde has also been reported, but these multistep processes are generally carried out in homogeneous phase and require the use of toxic reactants, such as halogenated compounds and strong acids and bases [5–7]. Moreover, the last step of this process, i.e. piperonyl alcohol oxidation, is achieved using a metal supported catalyst in a biphasic system. The solvent-free oxidation of isosafrole with supported $PhI(OAc)_2$ under microwave heating has been reported [8]; however the presence of iodobenzene acetate may raise safety concerns especially during the scale up process since hot spots can be produced during microwave irradiation. The synthesis of piperonal has also been reported in some patents: the use of both ferric nitrate and 4-hydroxy-2,2,4,4-methylpiperidine nitroxyl free rad-

* Corresponding authors at: Dipartimento di Scienza e Alta Tecnologia, University of Insubria, Via Valleggio 11, 22100, Como, Italy.
E-mail addresses: carlo.lucarelli@uninsubria.it, carlo.lucarelli2@unibo.it (C. Lucarelli).

http://dx.doi.org/10.1016/j.apcatb.2016.10.030
0926-3373/© 2016 Elsevier B.V. All rights reserved.

ical as catalysts for piperonyl alcohol oxidation, which is prepared from the piperonyl chloride, has been recently patented [9]. Furthermore, the reaction of piperonyl alcohol with oxygen in the presence of activated carbon and an amine compound was claimed as an efficient process to produce piperonal [10]. However, the above mentioned patents require the use of solvents and homogeneous co-catalysts.

Within the environmentally friendly processes, a photocatalytic route must be considered. Bellardita et al. have studied piperonyl alcohol oxidation in aqueous UV-irradiated TiO_2 suspensions, which resulted in a selectivity in piperonal of 35% [11].

Furthermore, recent works introduced the use of metal supported catalysts, like Pd/H-Beta and Pd or Pt supported on MgO, TiO_2, SiO_2 [12,13]. Unfortunately, the presence of $Pb(OAc)_2$, used as catalyst activator, and a sodium hydroxide solution make this process not attractive from the environmental point of view.

One of the most interesting supports to be used in alcohol oxidation reactions is CeO_2. As a matter of fact, cerium oxide is used as support in the preparation of many catalysts because its redox-properties and surface oxygen vacancies positively affect the catalytic activity [14,15]. Gold supported on ceria has been demonstrated to be very active and selective in the oxidation of alcohols to aldehydes. It is already known that catalytic properties are strictly related to the morphology and size of gold nanoparticles and their interaction with CeO_2 [16]. As reported by Corma et al. [17], CeO_2 surface area is another important property that plays a key role in catalytic performances; in particular, a strong collaborating effect between gold nanoparticles and ceria is able to promote alcohol oxidation [15]. Important results using Au supported on nanoceria have been described in the oxidation of allylic alcohol; this reaction has been carried out in a solventless ecofriendly process and gold guaranteed also a high chemoselectivity of the process with respect to other metals [18]. Gold catalysts have also been employed for benzyl alcohol oxidation reaction, which is often use as model reaction for the comparison of catalytic properties of new synthesized materials [19,20].

Furthermore, we reported on the importance of favoring gold-support interaction in ceria-based catalysts to enhance the catalytic activity in 5-hydroxymethylfurfural oxidation [21,22].

Considering the aforementioned drawbacks, an alternative synthetic route for piperonyl alcohol oxidation to piperonal was developed using Au/CeO_2 supported catalysts. This innovative methodology increases the atom efficiency, does not require any solvents or any toxic oxidant and it is performed under mild reaction conditions, using air as oxidant. Moreover, the effect of catalysts preparation on catalytic performance was investigated; in order to improve catalytic performance, high surface area ceria has been synthesized and gold nanoparticles were deposited over it both by preformed sol immobilization (I) and with the deposition precipitation (DP) method.

2. Experimental

2.1. Materials

$CeCl_3 \cdot 7H_2O$ (>99%), $Ce(NO_3)_3 \cdot 6H_2O$ (>99%), $CH_3(CH_2)_{11}OSO_3Na$ (>99%), NaOH, polyvinylpyrrolidone (PVP K25, m.w. 29,000), β-D-glucose, $HAuCl_4 \cdot 3H_2O$ (>99,9%), Lithium bis(trimethylsilyl)amide (LiHMDS) (97%), 0.1 M aqueous NaOH solution, toluene (CHROMASOLV® Plus, for HPLC, ≥99.9%), acetone (CHROMASOLV® Plus, for HPLC, ≥99.9%), 1,2,4-trimethylbenzene (>99%), benzyl alcohol (>99%) vanillyl alcohol (≥98%), anisyl alcohol (≥98%), 3,4-(Methylenedioxy)benzyl alcohol (or piperonyl alcohol, 98%), and undecane (>99%) were purchased from Sigma Aldrich and used without further purification. THF (Sigma Aldrich) was used immediately after drying over sodium-benzophenone under Ar atmosphere. The commercial CeO_2 used as support was purchased from Evonik (VP Ceria 60, Ce60).

2.2. Synthesis of the high surface area CeO_2

High surface area CeO_2 samples (hsCe) were synthesized by surfactant-template method, following a procedure similar to the one reported by Guo et al. [23] using two different cerium precursors, $CeCl_3 \cdot 7H_2O$ and $Ce(NO_3)_3 \cdot 6H_2O$ (hsCe_Cl and hsCe_NO3). Cerium precursor (27.00 mmol) was completely dissolved in distilled water (270 mL) and added dropwise to a water (105 mL) solution of dodecyl sodium sulfate (73.00 mmol). The obtained mixture was kept under vigorous stirring for 30 min, when a homogeneous and transparent microemulsion was obtained. Then a solution (160 mL) of NaOH (4.6 g) was added gradually. After 6 h at RT under vigorous stirring, Ce ions have been precipitated within the micelles; at this point, the mixture was transferred into a sealed vessel and submitted to microwave-hydrothermal treatment (110 °C 2 h, rate 2 °C/min, 800 W) using a Milestone Start-SYNTH microwave unit. The yellow precipitate was filtered, washed several times with water and ethanol, dried at 90 °C overnight and calcined at 300 °C for 2 h (rate 2 °C/min).

2.3. Synthesis of Au colloids

Au colloids were prepared by means of Au(III) reduction with glucose in alkaline water in presence of PVP as stabilizing agent [24]. PVP (158 mg, 1.39 mmol) and NaOH (161 mg, 4.03 mmol) were dissolved in 90 mL of distilled water and the solution was heated under vigorous stirring at 95 °C. Once this temperature has been reached, an aqueous solution (10 mL) of $HAuCl_4 \cdot 3H_2O$ (198 mg, 0.50 mmol) and β-D-glucose (181 mg, 1.01 mmol) was quickly added to the flask, and stirred for 2.5 min. After reaction, a deep red stable suspension of Au NPs was obtained.

2.4. Catalysts preparation

Gold supported catalysts were prepared using both the home-made high surface area CeO_2 and the commercial one (Evonik, VP ceria 60). Gold was deposited on the two considered CeO_2 supports, using two different methods: (i) immobilization of the preformed colloids, and (ii) deposition-precipitation using four different metal weight ratios (0.3, 0.5, 1.0 and 5.0 wt.%).

(i) *Immobilization of preformed colloid* (labeled I in the following sections). The samples were prepared by incipient wetness impregnation of CeO_2 using the colloids prepared by Au(III) reduction with glucose as indicated elsewhere [24]. The catalysts were dried at 120 °C overnight and calcined at 300 °C for 2 h (rate 2 °C/min).

(ii) *Deposition precipitation* [25] (labeled DP in the following sections). The pH of an aqueous solution of $HAuCl_4 \cdot 3H_2O$, 1.10^{-3} M, was adjusted to 8 by adding dropwise a 0.1 M NaOH solution. Similarly, the pH of an aqueous suspension (300 mL) of 2 g of CeO_2 was brought to 8. The gold solution was then added dropwise to the ceria suspension under vigorous stirring at room temperature (r.t.) and the stirring continued for 2 h at 65 °C. This procedure resulted in the selective deposition of $Au(OH)_3$ on the ceria surface. The pH of the mixture was continuously monitored and kept constant at 8. The mixture was sonicated for 15 min in an ultrasonic bath. Then, the solid was filtered, washed several times with water to remove chloride, dried at 110 °C overnight and calcined at 300 °C for 2 h (rate 2 °C/min).

Table 1
List of prepared samples reporting preparation method, theoretical and measured metal load (by ICP) and BET surface area.

Sample name	Gold deposition	Metal load (wt.%)		Surf. area (m^2/g)
		Theoretical	*ICP-MS*	
Ce60	Commercial CeO_2	–	–	53
Ce60_I_03	Sol Imm.	0.3	0.22	54
Ce60_I_05	Sol Imm.	0.5	0.45	52
Ce60_I_1	Sol Imm.	1.0	0.93	55
Ce60_I_5	Sol Imm.	5.0	4.88	53
Ce60_DP_03	Dep. Precip.	0.3	0.26	52
Ce60_DP_05	Dep. Precip.	0.5	0.47	54
Ce60_DP_1	Dep. Precip.	1.0	0.97	55
Ce60_DP_5	Dep. Precip.	5.0	4.93	51
hsCeCl	Nano CeO_2 from Chloride	–	–	222
hsCeCl_I_05	Sol Imm.	0.5	0.41	216
hsCeCl_DP_05	Dep. Precip.	0.5	0.45	223
hsCeNO3	Nano CeO_2 from Nitrate	–	–	220
hsCeNO3_I_05	Sol Imm.	0.5	0.46	217
hsCeNO3_DP_05	Dep. Precip.	0.5	0.44	220

The following abbreviations are used to identify the catalysts: Ce60 denotes the commercial CeO_2; hsCe denotes the high surface CeO_2, which may be followed by Cl or NO_3, depending on the precursor; I denotes immobilization; DP denotes deposition-precipitation; and finally the numbers (0.3, 0.5, 1.0, 5.0) denote the gold loading (wt.%). Details on the characteristics of the prepared catalysts are reported in Table 1.

2.5. Catalyst characterization

2.5.1. BET specific surface area

The BET surface area of the catalysts was determined by nitrogen absorption at the temperature of liquid nitrogen using a Sorpty 1750 Fison Instrument. 0.3 g of powder were typically employed for the measurement and the sample was outgassed at 150 °C before N_2 absorption.

2.5.2. High resolution transmission electron microscopy (HR-TEM)

HR-TEM images were recorded using a TEM/STEM FEI Tecnai F20 working at 200 KeV. The crystal plane spaces, Fast Fourier Transform (FFT) rings and Inverse Fast Fourier Transform (IFFT) patterns were obtained through analyzing the TEM micrographs using the Gatan Digital Micrograph software. Data about crystal plane space were obtained by the techniques of FFT, applying masks, invert FFT transform, which is the base for determining crystal phases by comparison with the standard ICDD-PDF data.

2.5.3. ICP-MS

Solid catalyst dissolution was achieved by microwave assisted digestion (Milestone MEGA 1200) in 2 mL of pure HF (Fluka TraceSelect ≥ 49%); the latter was subsequently removed by evaporation before analysis. Impregnation solutions were syringe filtered (0.45 μm pore size) and adequately diluted before analysis. Gold determinations were performed by Inductively Coupled Plasma – Mass Spectrometry (ICP-MS): X-SeriesII ICP – MS from Thermo Elemental was used. Instrumental settings were adjusted as suggested by the manufacturer; major instrumental parameters are as follows: plasma power 1.4 kW; gas flows: nebuliser 0.97 L/min, cool 13.00 L/min and auxiliary 1.00 L/min. External calibration was used for quantification using the $m/z = 197$ signal.

2.5.4. Thermogravimetric/differential thermal analyses (TGA/DTA)

TGA/DTA analyses were performed over fresh and spent catalysts in order to identify the amount of high molecular mass compounds absorbed over the catalyst surface using a SDT Q 600 instrument. A sample of 5–10 mg was typically employed and the temperature was programmed from r.t. to 900 °C with an heating rate of 10 °C/min in air.

2.5.5. Temperature programmed reduction (TPR)

The reduction behavior was studied by Temperature Programmed Reduction using a Micromeritics AutoChem II Chemisorption Analyser TPDRO instrument under 5% H_2/Ar flow (20 mL/min). The temperature was raised from 60 to 650 °C with a heating rate of 10 °C/min followed by an isothermal step at 650 °C for 30 min. Prior to the experiment, samples were pretreated for 30 min in an 5% O_2/He mixture (20 mL/min) at 300 °C.

Raman analyses were performed on spent samples (i.e. samples unloaded after reaction) using a Renishaw 1000 instrument equipped with a Leica DMLM microscope equipped with a laser diode source (780 nm); before measurements the spent samples were heated under vacuum at 100 °C to desorb the organic compounds physically adsorbed.

2.6. Catalytic tests

The alcohols oxidation reactions were carried out in a magnetically stirred glass semi-batch reactor.

The oxidation tests were performed in the presence of toluene as solvent at 100 °C, at atmospheric pressure by bubbling air through the slurry (20 mL/min). Typically 180 mg of the catalyst were suspended in a toluene solution (10 mL) of 4.6 mmol of the alcohol and 4.6 mmol of 1,2,4-trimethylbenzene. The latter is chemically inert in the used conditions and was added to correct the effect of the solvent stripping. Moreover, cooled trap filled with toluene was connected to the reactor in order to collect all the molecules stripped out by the gas flow. The solution in the trap was analyzed and the amount of product was evaluated for the reactant conversion and products yields calculations. Considering that the total amount of 1,2,4-trimethylbenzene used was found either in the reactor or in the trap, we had the proof that even reactant and products were completely recovered, since 1,2,4-trimethylbenzene has got lower molecular weight and lower boiling point.

The resulting mixture was heated at 100 °C for 4 h and air was bubbled continuously trough the suspension. After the reaction the catalyst was separated by centrifugation (1500 rpm for 10 min) and the products were analyzed by Carlo Erba 4300 gas chromatograph, equipped with FID and a HP-5 column (length 30 m, i.d. 0.32 mm, film width 0.25 μm) and identified by GC–MS analysis using an AgilentTechnology 6890N equipped with a 5973 mass selective detector and an HP5 column (length 25 m, i.d. 0.25 mm, film width

1.5 μm). Product concentrations were calculated by GC analysis using undecane as internal standard.

Solvent free oxidation tests were also performed in this kind of reactor using piperonyl alcohol, vanillyl alcohol and anisyl alcohol as substrates. Typically 1,5 g of the alcohol was introduced inside the reactor with 390 mg of the catalyst; the resulting mixture was heated at atmospheric pressure at 120 °C for 4 h and air was bubbled continuously trough the suspension (30 mL/min). During these tests the ratio substrate:Au was fixed at a value of 1000 (mol/mol). After the reaction, the slurry was dissolved in acetone and the catalyst separated by centrifugation. The products were analyzed by HPLC, using an Agilent Technologies 1260 Infinity instrument equipped with a DAD UV–vis detector and a Agilent POROshell 120 C-18 column.

For the catalytic test carried out under pressure a 100 mL Parr Instruments autoclave reactor was used, following this procedure: the reactor was charged with 25 g of toluene as solvent, 0,5 g of the substrate and the catalyst (substrate/Au molar ratio = 1000). The autoclave was purged 3 times with O_2 (5 bar) and then pressurized at 10 bar. The temperature was increased to 120 °C and the reaction mixture was stirred at approximately 400 rpm for 4 h. At the end of the reaction, the reactor was cooled down to room temperature and the solution was filtered and the products were analyzed as indicated above.

3. Results and discussion

3.1. Catalysts characterization

According to the current research status, the preparation of Au catalysts with controlled size over nano-CeO_2 may be a promising way to produce catalysts with high activity and selectivity for the reaction of piperonyl alcohol oxidation [26]. On this prospective, a very reproducible synthesis of nano-ceria was developed, aimed at obtaining high surface area materials with a simple microwave-assisted procedure, suitable for industrial application, in contrast to demanding synthetic strategies previously reported in literature [27].

High surface CeO_2 (hsCe) was successfully prepared using two different cerium precursors, $CeCl_3$ (hsCeCl samples) and $Ce(NO_3)_3$ (hsCeNO3 samples) by a surfactant-template method following a procedure similar to the one reported by Guo et al. [23]. BET surface area of these samples is 222 and 220 m^2/g, respectively (Table 1), owing to their nanometric crystal size; these values are significantly higher than that of the commercial support (VP Ceria 60 Evonik = 53 m^2/g).

Gold was added to the supports by two different methods: i) Immobilization of preformed metal sol and ii) Deposition-Precipitation. Both these strategies resulted in the quantitative deposition of the metal over the supports, as demonstrated by ICP-MS analysis (Table 1); small discrepancy between theoretical and experimental amounts is in the range of experimental error. In any case, gold deposition did not cause a significant decrease of surface area, indicating that metal insertion did not give rise to a significant change in the total porosity.

Fig. 1 shows selected HR-TEM observations on Au/CeO_2 catalysts prepared using commercial and hsCeCl ceria.

The crystallites of commercial ceria are inhomogeneous with dimension in the range 8–40 nm (Fig. 1a–b–c). On the contrary, homemade CeO_2 (Fig. 1d–e) is characterized by quasi-spherical particles of fairly uniform size (4 nm). Au species dispersion over ceria is strongly related to the method utilized for catalyst preparation and to ceria surface area (Figs. 1 and 2). Indeed, supported Au nanoparticles obtained by sol immobilization retain the size and distribution of pristine gold nanosol after drying (4–5 nm; Figs. S1–S2) but show an increase in the dimension after calcination at 300 °C (7–8 nm), independently from ceria surface area and gold content.

This confirms that the preparation of Au/CeO_2 by deposition of preformed nanoparticles is not support-dependent and that Au nanoparticles slightly sinter after thermal treatment, due to organic stabilizing agent combustion [21].

On the contrary, metal dispersion over catalysts synthetized by DP was strongly dependent on metal content and ceria surface area (commercial ceria Ce60 vs homemade hsCeCl). Indeed, Ce60_DP_05 (0.5 wt.%) was characterized by a sharp Au dimensional distribution centered at 3 nm. Ce60_DP_5 (5.0 wt.%) shows gold agglomeration, leading to bimodal distribution where the small and homogeneous size observed at low metal content was lost, with the formation of discrete metallic particles up to 12–14 nm.

Hence, catalyst prepared by DP method on the synthesized nanoceria is characterized by the smallest particle size distribution. Gold nanoparticles obtained by DP on homemade supports were very hardly visualized by HR-TEM, due to the fact that dimensions of both gold and ceria particles are in the range of few nanometers. In fact XRD analyses did not revealed the any peak attributed to gold, while ICP-MS analyses confirmed the presence of gold as reported in Table 1. Nevertheless, the combination of HR-TEM imaging and SAED demonstrated that this synthesis resulted in the formation of very small Au nanoparticles, with size of about 1 nm (Fig. 2, gray rectangle).

It is well known that, in the presence of Au, the oxygen storage capacity of CeO_2 may increase, facilitating the superficial Ce^{4+} reduction. Therefore, the effects of gold deposition on CeO_2 were investigated using H_2-TPR. Typically, the TPR profile of pristine CeO_2 is characterized by reduction peaks at 450–500 °C and 800 °C, which may be ascribed to the surface capping oxide ions and to the bulk oxygen, respectively [22,28,29].

However, the reducibility of pristine cerium oxide is strongly dependent on its crystal size. Indeed, the reduction peak for homemade ceria surface ions shifted to a significantly lower temperature (400 °C) compared to the commercial Ce60 sample (550 °C) (Fig. S3).

On the contrary, gold containing samples show the presence of intense peaks at temperatures well below the pristine supports. As a matter of fact, size and dispersion of gold nanoparticles which determine the redox properties of catalysts, depend on the used synthetic approach (Fig. 3).

Focusing the attention on samples prepared using commercial CeO_2 (Fig. 3, sample b, c, e), it is possible to observe that preformed gold nanoparticles (Ce60_I_0.5 sample), which are sized in the range of 7–8 nm, lead to lower ceria reduction compared to DP samples (Ce60_DP_0.5 and Ce60_DP_5). In fact, the presence of smaller and more reactive gold particles promotes Ce^{4+} reduction. However, since the difference in the particle size of the considered samples is in the range of a few nanometers, the temperature shift is not so relevant. Moreover, high amount of gold leads to a very broad particle size distribution. Indeed, the reduction profile of Ce60_DP_5 sample shows a maximum centered at about the same temperature of Ce60_DP_05 material but with significantly lower H_2 consumption. In this case, two effects have to be considered: the higher amount of gold leads to a lower reduction temperature, whereas broaden particles size distribution makes Ce^{4+} reduction more difficult.

The use of high surface area CeO_2 (Fig. 3, sample a and d) leads to the formation of a very broad reduction peak, centered at 300 °C, in the case of preformed Au sol (hsCeCl_I_05 sample). On the contrary, the synthesis by DP significantly decreases the temperature of Ce^{4+} reduction and strongly increased the amount of H_2 consumed. This behavior may be ascribed to the increase of gold-support interaction in the hsCeCl_DP_05 sample. As a matter of fact, this sample shows extended surface area and presence of a high number of very

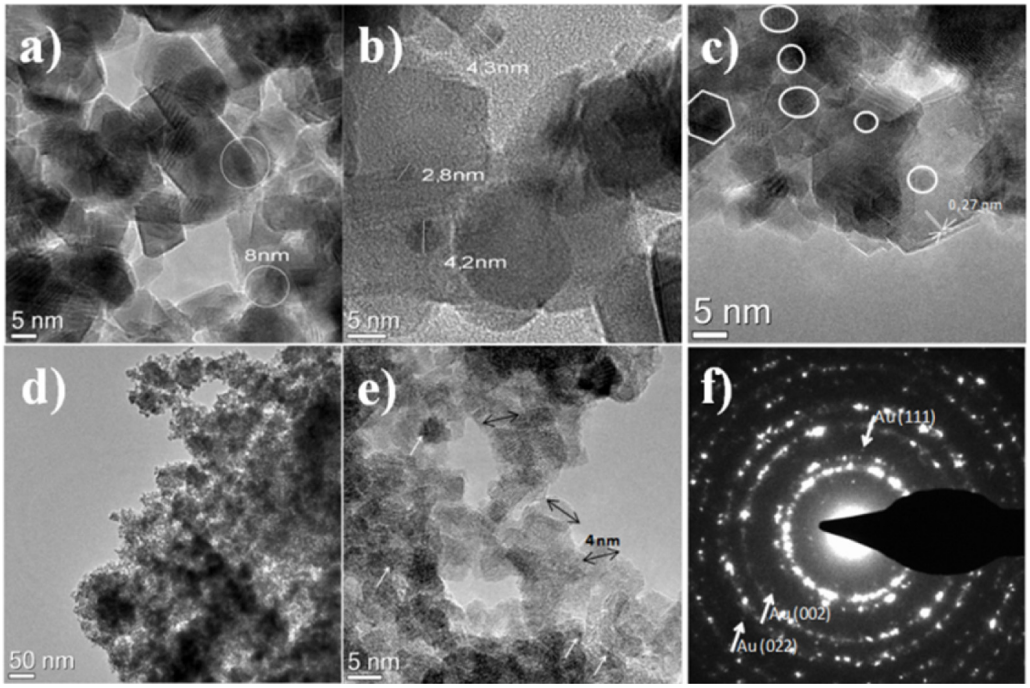

Fig. 1. Representative HR-TEM images showing samples: a) Ce60_I_05; b) Ce60_DP_05; c) Ce60_DP_5; d) & e) hsCeCl_DP_05; f) SAED pattern for hsCeCl_DP_05.

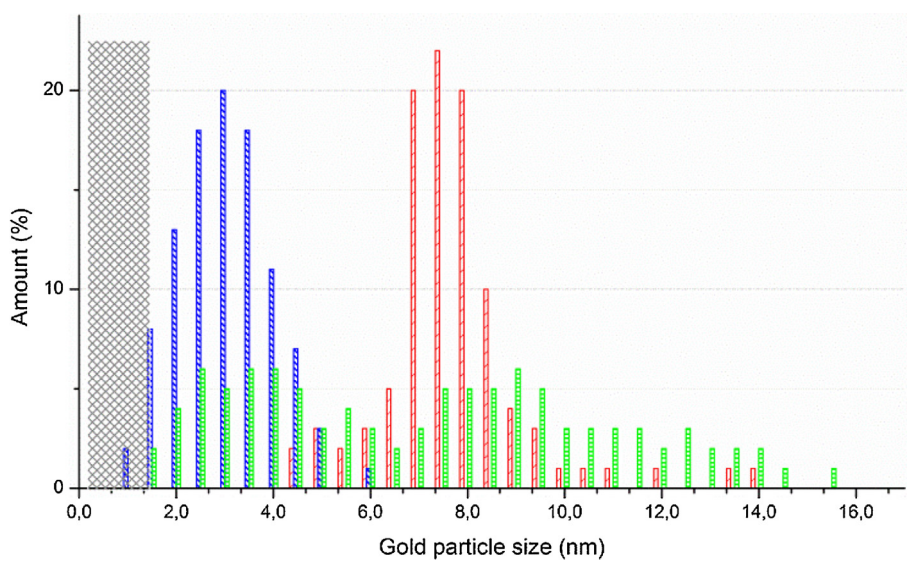

Fig. 2. Au size distribution histograms for different Au/CeO_2 samples. Legend: hsCeCl_DP_05 ( ),Ce60_DP_05 ( ), Ce60_I_05 ( ),Ce60_DP_5 ( ).

small gold nanoparticles, which result in a higher surface reactivity of Ce^{4+} sites. They are more likely to be reduced thanks to the enhanced interaction that takes place in the presence of smaller gold nanoparticles and high surface area nanoceria.

3.2. Catalytic tests

Considering the high amount of papers published on benzyl alcohol oxidation and gold supported catalysts, preliminary tests using this model reaction were carried out in order to correlate results with literature and select the best synthetic procedure to prepare the catalyst.

Two different methods of supporting gold were studied using commercial CeO_2 and high surface area nanoceria prepared by microemulsion. Gold was deposited as preformed nanoparticles (I) or by deposition precipitation (DP) in different amount. The results obtained with these two series of samples highlighted that nanoceria prepared by microemulsion is more active than the commercial one especially when DP method was used (see Supplementary). An improvement of catalytic activity was observed for low metal loading since particle dispersion was favoured; for this reason, 0.5%wt was chosen as metal loading for the preparation of catalyst. All the above mentioned results show that the most active catalyst in benzyl alcohol oxidation is the one prepared with high surface area nanoceria with the DP method (hsCeCl_DP). Therefore, this catalyst was used for piperonyl alcohol oxidation. However, the differences in the catalytic activity of piperonyl alcohol oxidation correlated both to different types cerium oxide (hsCeCl_DP and Ce60_DP) and to different gold deposition methods: (Ce60_DP and Ce60_I) were studied. Gold supported on the high surface area CeO_2

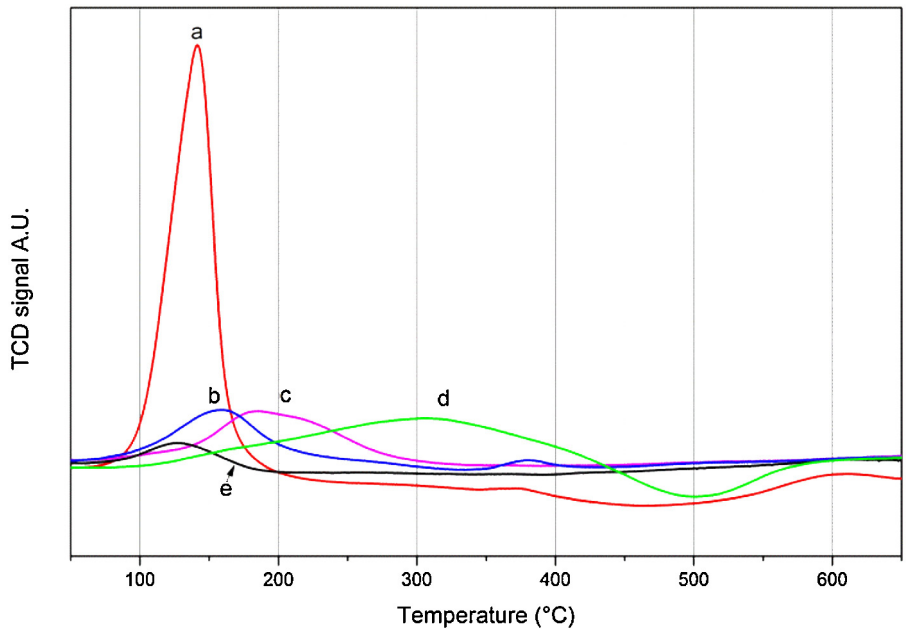

Fig. 3. H_2-TPR profiles of the different samples; a) hsCeCl_DP_05; b) Ce60_DP_05; c) Ce60_I_05; d) hsCeCl_I_05; e) Ce60_DP_5.

Table 2
Catalytic activity of hsCeCl_DP_05, Ce60_DP_05 and Ce60_I_05 in piperonyl alcohol oxidation. Reaction conditions: solvent toluene, 4.6 mmol benzyl alcohol, 180 mg catalyst, 100 °C in bubbling air (20 mL/min), 4 h.

Catalyst	Piperonyl alcohol conv. (%)	Piperonal Yield (%)	Piperonal Sel. (%)
hsCeCl_DP	61	47	78
Ce60_DP	39	32	82
Ce60_I	36	30	85

sample prepared by deposition-precipitation (hsCeCl_DP) exhibited the highest activity being the most active catalyst (Table 2), as already seen in benzyl alcohol oxidation. In all tests, piperonal has been detected as only product of the reaction, but selectivity values suggest that some by-products in hardly detectable amounts were probably produced. The possibility to increase piperonyl alcohol conversion was demonstrated by carrying out a catalytic test under oxygen pressure in autoclave reactor. The use of high oxygen pressure in the oxidation process led to an increase in piperonal yield up to 81%, while the selectivity remained 100%.

The main target of the present work was not to obtain the complete conversion of the alcohol into the aldehyde but tuning an eco-friendly and industrially attractive way to produce piperonal or other aromatic aldehydes by oxidation of the corresponding alcohols. Therefore, since the initial promising results in benzyl alcohol oxidation were confirmed in the oxidation of piperonyl alcohol we carried on the study of this process using the optimized hsCeCl_DP_05 catalyst under diluted and solvent free reaction conditions.

The catalytic activity of hsCeCl_DP_05 sample was first tested in the oxidation of piperonyl alcohol with air in a toluene solution. The results are presented in Fig. 5. Catalyst shows a high efficiency in the oxidation and Au supported on nano-CeO_2 is very selective in piperonal formation, yielding 46% of the aldehyde after 4 h or reaction. Small amounts of piperonyl acid and ester are found in this condition and maximum of 80% selectivity is obtained.

Successively, the oxidation was performed using the pure substrate, i.e. solvent free, to make the process greener and more affordable with respect to existing procedures. Solvent free conditions show very interesting performance (Table 3). Indeed, even if the conversion slightly decreases, the selectivity to piperonal, in the absence of the solvent, resulted higher than 99% due to the fact that in this condition the fconsecutive products are not formed. This is an outstanding result, which may be strongly beneficial for an industrial application. In fact, the absence of organic solvent in the reaction and the complete selectivity to the desired product significantly reduce the costs of the purification section in the process.

In order to further improve the performance of the process, a catalytic test using oxygen instead of air was performed (Table 3) with the aim of increasing alcohol conversion without worsening the selectivity. As expected, the influence of the higher oxygen concentration is very strong and the conversion increases from 46% to 68% without any selectivity reduction.

We subsequently investigated the effect of temperature and reaction time on piperonyl alcohol oxidation (Table 4). The tests demonstrate the possibility to reach total alcohol conversion increasing temperature and reaction time, although with a marked decrease in piperonal selectivity is observed. Indeed, higher temperature and increased reaction time favour the formation of piperonyl acid and ester, as confirmed by NMR analysis (See supplementary). Therefore, the obtained results seem to suggest that the reaction network consists in the rapid transformation of piperonyl alcohol to piperonal, which at high temperature and long reaction time, partially oxidizes forming the acid. Subsequently, as also observed for benzyl alcohol oxidation, piperonylic acid can easily reacts with the alcohol, leading to the formation of the ester as reported in Scheme 1.

3.3. Catalyst stability and reusability

Since catalyst stability is fundamental from the industrial point of view, reusability tests were carried out with the Au/CeO_2 catalyst. In each test cycle, piperonyl alcohol oxidation is studied in

Table 3
Catalytic activity of hsCeCl_DP_05 in piperonyl alcohol oxidation. Reaction conditions: molar ratio piperonyl alcohol/gold = 1000, 120 °C, 4 h, bubbling air or O_2 (30 mL/min).

Solvent	Pressure/Oxidant	Piperonyl alcohol conv. (%)	Piperonal Yield (%)	Piperonal Sel. (%)
Toluene	Ambient/air	61	47	78
–	Ambient/air	46	46	100
–	Ambient/O_2	68	68	100

Table 4
Effect of reaction time and temperature. Reaction conditions: molar ratio piperonyl alcohol/gold = 1000, bubbling O_2 (30 mL/min), solvent free. Catalyst: hsCeCl_DP_05.

T (°C)	Reaction time (min)	Piperonyl alcohol conv. (%)	Piperonal Yield (%)	Piperonal Sel. (%)	Others
120	240	68	68	100	–
150	240	91	84	93	7
150	360	95	83	88	12

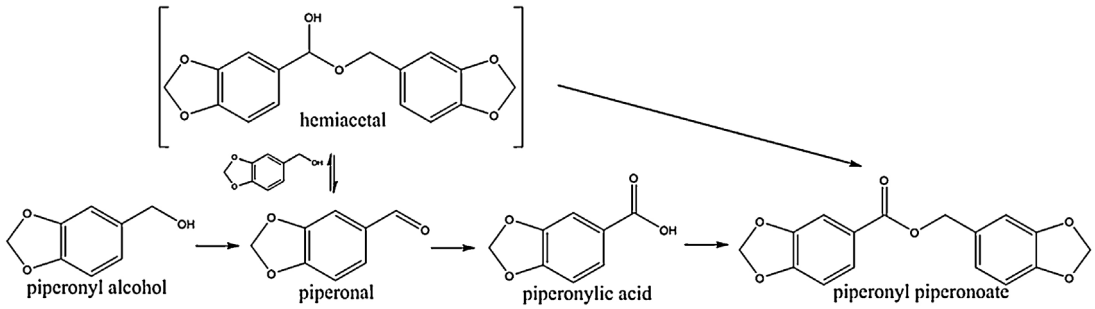

Scheme 1. Reaction scheme for piperonyl alcohol oxidation.

solvent-free conditions with the catalyst recovered by filtration, washing by acetone, followed by drying (120 °C, 2 h).

Fig. 4 shows the four cycles of catalyst used and recovered, obtained on different samples (hsCe_DP_05, Ce60_DP_05 and Ce60_I_05). These results indicate that a rapid deactivation occurs for all the studied materials being the deactivation more evident for catalysts with the higher activity. Nevertheless, chemical analysis of the filtered shows the absence of gold leached out during the four cycles, confirming the stability of synthetized structures in the studied reaction conditions.

Based on the TGA/DTA and Raman results reported in Fig. 5, this decreased activity may be ascribed to the absorption of some oligomers and carbonaceous compounds on the catalyst surface. Indeed, the thermogravimetric profile of used hsCeCl_DP_0.5 catalyst—performed by heating samples from r.t. 800 °C in air—indicates a significant weight loss at 200 °C, associated to a strong exothermic peak. Moreover, Raman studies on used catalysts indicate the presence of bands due to organic compounds adsorbed on the surface (insert in Fig. 5).

To verify the possibility to recover the activity of Au/CeO_2 samples, the regeneration by thermal treatment of used powders was investigated. After the oxidation reaction, the catalyst is recovered and thermally treated for 2 h at 400 °C in air. It has been verified that the thermal treatment at temperature higher than that used for catalysts preparation does not change gold particle size and catalyst morphology. Fig. 6 compares piperonyl alcohol conversion and piperonal selectivity for fresh, used and regenerated hsCeCl_DP_05 catalysts. The regeneration treatments led to a significant recovery of piperonyl alcohol activity when catalyst was treated at 400 °C confirming the deactivation to be connected to the organic compound absorbed on the catalyst. This treatment allowed the catalyst to remain active even after the fifth consecutive reaction and regeneration at 400 °C, without showing a decrease in piperonyl alcohol conversion, due to catalyst deactivation. Moreover, piperonal selectivity is not affected by the regeneration treatments confirming that the observed catalyst deactivation can be overcome using a regeneration treatment.

The typical observed kinetic profile for the oxidation of piperonyl alcohol using the hsCeCl_DP_05 catalyst is reported in Fig. 7. This curve indicates the presence of a rapid increase of conversion in the first hour of reaction, followed by approximately steady state conditions. The alcohol rapidly transforms in piperonal with selectivity in excess of 99% during the first period of reaction whereas the piperonal yield is almost unchanged between 60 and 240 min, suggesting the presence of a significant deactivation of the catalysts after 30–45 min of reaction. This phenomenon may be ascribed to the formation of esters from produced piperonal, which adsorbs over the surface of the catalyst. Nevertheless, the results indicate that these oligomers start to form just when a significant amount of piperonal is present in the reaction medium. Therefore, to verify the possibly to control the catalyst deactivation, stopping the reaction before the starting of oligomers formation, we performed some oxidation reactions, arresting tests at 15 and 30 min and reloading the catalyst after filtration and drying. The obtained results (Fig. 7) confirm the stability of the materials in this condition, proving the possibility to design an oxidation process to produce piperonal by piperonyl alcohol oxidation, with high selectivity over the developed hsCeCl_DP_05 catalyst.

Therefore, from the industrial point of view, it could be possible to scale up the process using a low reaction time batch reactor or low conversion continuous reactor. In the latter case, if fixed bed reactor is used, catalyst regeneration could be done in situ.

To demonstrate the general applicability of the hsCe_DP_05 catalyst in the selective oxidation of aromatic alcohols to the relative aldehydes, we tested this material in the oxidation of vanillyl and anisyl alcohols (Table 5).

The catalyst is equally effective for the oxidation of these substrates and forms the aldehyde as the main product in both cases, confirming the wider applicability of prepared Au/CeO_2 catalyst. Using these raw materials, the conversion was higher with respect to piperonyl alcohol, probably because of the different steric hindrance of vanillyl and anisyl alcohol although the selectivity was slightly lower. Additional products formed are identified as acids and esters. Nevertheless, the fine-tuning of the reaction conditions,

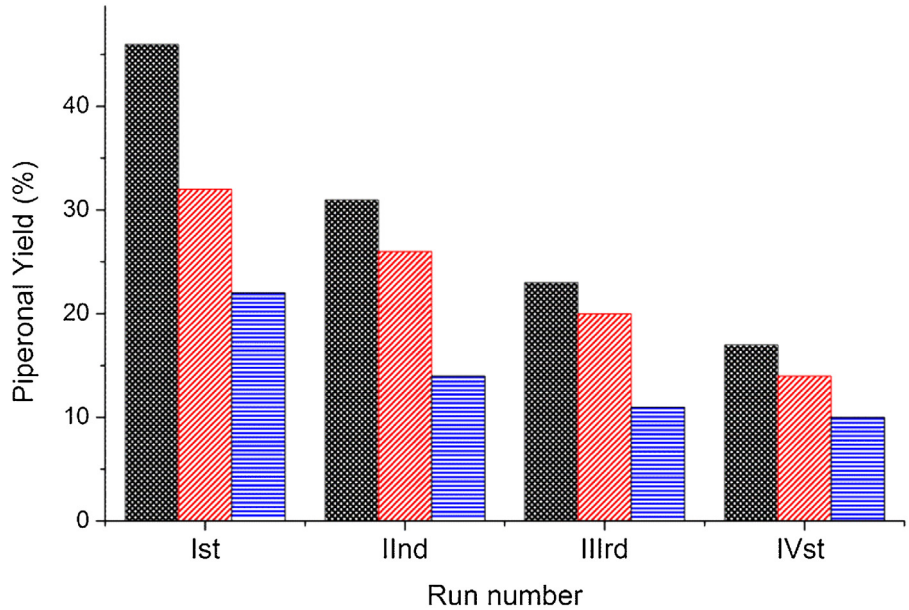

Fig. 4. Reusability study in the oxidation of piperonyl alcohol using different catalysts. Reaction conditions: molar ratio piperonyl alcohol/gold = 1000, 120 °C, 4 h, bubbling air (30 mL/min), solvent free. Legend: ■ hsCeCl_DP_05; ■ Ce60_DP_05; ■ Ce60_I_05.

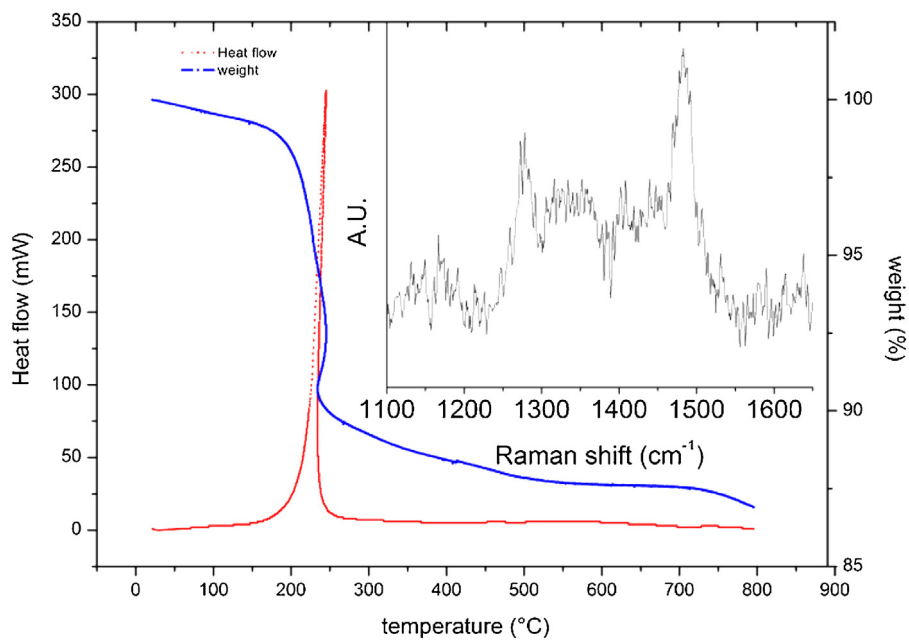

Fig. 5. Termogravimetric (TGA) and differential thermal analysis (DTA) of the used hsCeCl_DP_05. Inset: Raman spectra of used hsCeCl_DP_05.

Table 5
Oxidation of vanillyl and anysil alcohol with hsCeCl_DP_05 catalyst. Reaction conditions: molar ratio alcohol/gold = 1000, 120 °C, bubbling air (30 mL/min air), solvent free, reaction time 4 h.

Alcohol	Alcohol conv. (%)	Aldehyde Yield (%)	Aldehyde Sel. (%)	Others
Vanillyl alcohol	76	70	92	8
Anisyl alcohol	82	71	87	13

for now well optimized for the synthesis of piperonal, can increase the selectivity also in the oxidation of different alcohols.

4. Conclusions

High yield values in pure piperonal and other aromatic aldehydes, were obtained by selective oxidation of the corresponding alcohols using an economic and sustainable approach. The reactions, characterized by 100% atom efficiency, were performed under solvent-free conditions, using heterogeneous catalysts and air at atmospheric pressure. In particular, highly dispersed nano-Au particles supported on nano-CeO_2 were able to catalyse the formation of piperonal without any by-products formation. The fine-tuning of reaction conditions demonstrated the possibility to

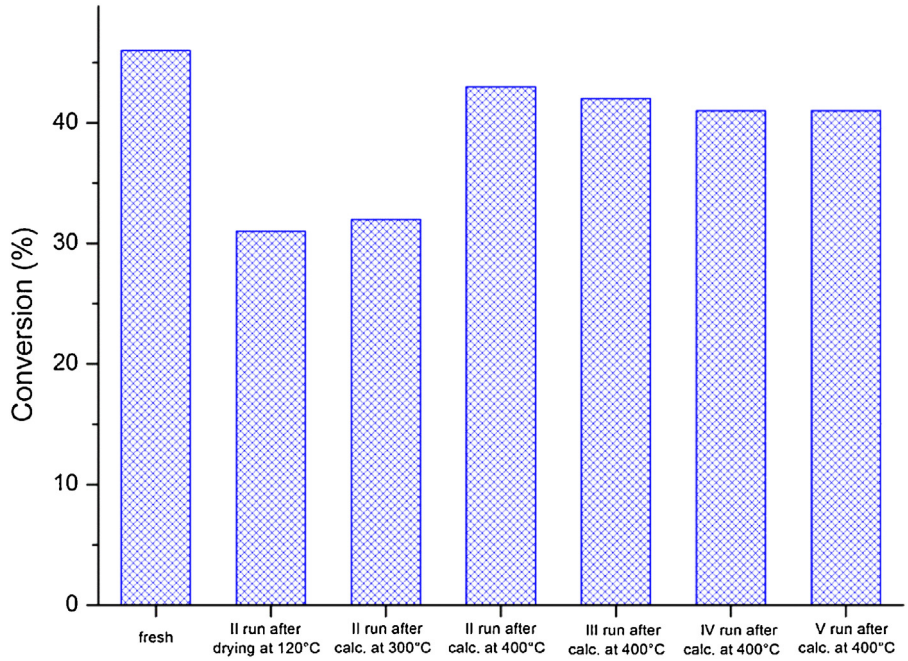

Fig. 6. hsCeCl_DP_05 reusability study in piperonyl alcohol oxidation. Results are given at total selectivity in piperonal. Reaction conditions: molar ratio piperonyl alcohol/gold = 1000, 120 °C, 4 h, bubbling air (30 mL/min), solvent free.

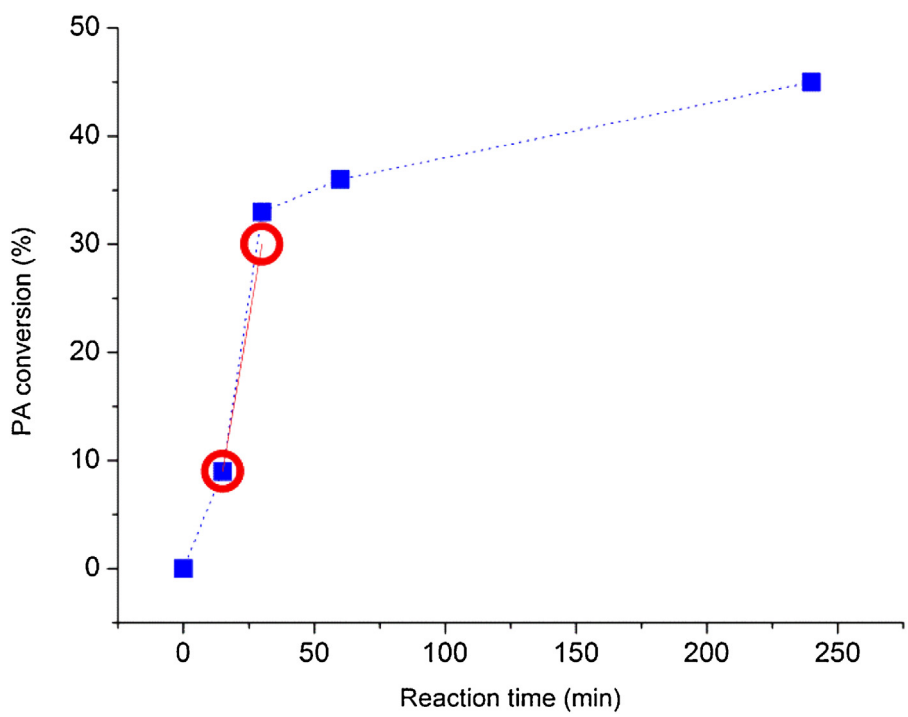

Fig. 7. Effect of the reaction time on piperonyl alcohol conversion using hsCeCl_DP_05 catalyst. Reaction conditions: molar ratio piperonyl alcohol/gold = 1000, 120 °C, bubbling air (30 mL/min), solvent free. Legend: ■ fresh catalyst; O used catalyst.

control catalyst deactivation, mainly associated to the adsorption, over the catalysts surface, of oligomers formed at high alcohol conversion.

References

[1] M. Zviely, Aroma Chemicals, In Kirk-Othmer Encyclopedia of Chemical Technology, John Wiley & Sons, N.Y (USA), 2002.
[2] N.T. Farinacci, US Patent 2, 794, 813, (1957).
[3] H.E. Mais, US Patent 3799940 (1974) assigned to Emery Industries Inc.
[4] Interchemical Corporation, GB Patent 1092615 (1967).
[5] Mitsui Toatsu Chemicals, French Patent 2412541, (1979).
[6] K. Nakatani, T. Inoue, T.S.N. Nishizawa, T. Ishii, US Patent 4157333, (1979) assigned to Mitsui Toastu Chemicals Inc.
[7] V. Borzatta, E. Capparelli, C. Gobbi, E. Poluzzi, WO Patent 042,512 (A1), 2005 assigned to Endura.
[8] H.M. Alvarez, D.P. Barbosa, A. Tinoco Fricks, D.A.G. Aranda, R.H. Valdeís, O.A.C. Antunes, Org. Process Res. Dev. 10 (5) (2006) 941–943.
[9] L. Dongfeng CN Patent 103, 936, 709, 2014.

[10] S. Masashi, M. Shuji, JP Patent 207, 797, 2011.
[11] M. Bellardita, V. Loddo, G. Palmisano, I. Pibiri, L. Palmisano, V. Augugliaro, Appl. Catal. B: Environ. 144 (2014) 607–613.
[12] O.P. Tkachenko, L.M. Kustov, A.L. Tarasov, K.V. Klementiev, N. Kumar, D.Yu Murzin, Appl. Catal. A: Gen. 359 (2009) 144–150.
[13] A.L. Tarasov, L.M. Kustov, A.A. Bogolyubov, A.S. Kiselyov, V.V. Semenov, Appl. Catal. A: Gen. 366 (2009) 227–231.
[14] N. Pal, E.-B. Cho, D. Kim, RSC Adv. 4 (2014) 9213–9222.
[15] A. Abad, P. Concepcion, A. Corma, H. Garcia, Angew. Chem. Int. Ed. 44 (2005) 4066–4069.
[16] A. Abad, A. Corma, H. Garcia, J. Chem. Eur. 14 (2008) 212–222.
[17] S. Carrettin, P. Concepción, A. Corma, J.M. López Nieto, V.F. Puntes, Angew. Chem. Int. Ed. 43 (2004) 2538–2540.
[18] A. Abad, A. Corma, H. García, Pure Appl. Chem. 79 (11) (2007) 1847–1854.
[19] D.I. Enache, D.W. Knight, G.J. Hutchings, Catal. Lett. 103 (2005) 43–52.
[20] M. Alhumaimess, Z. Lin, W. Weng, N. Dimitratos, N.F. Dummer, S.H. Taylor, J.K. Bartley, C.J. Kiely, G.J. Hutchings, ChemSusChem 5 (2012) 125–131.
[21] S. Albonetti, A. Lolli, V. Morandi, A. Migliori, C. Lucarelli, F. Cavani, Appl. Catal. B: Environ. 163 (2015) 520–530.
[22] A. Lolli, R. Amadori, C. Lucarelli, M.G. Cutrufello, E. Rombi, F. Cavani, S. Albonetti, Microporous Mesoporous Mater. 226 (2016) 466–475.
[23] M.-N. Guo, C.-X. Guo, L.-Y. Jin, J.-Y. Wang, J.-Q. Lu, M.F. Luo, Mater. Lett. 64 (2010) 1638–1640.
[24] T. Pasini, M. Piccinini, M. Blosi, R. Bonelli, S. Albonetti, N. Dimitratos, J.A. Lopez-Sanchez, M. Sankar, C.J. Kiely, G.J. Hutchings, F. Cavani, Green Chem. 13 (2011) 2091–2099.
[25] U.R. Pillai, S. Deevi Appl, Catal. A: Gen. 299 (2006) 266–273.
[26] A. Corma, Angew. Chem. Int. Ed. 44 (2005) 4066–4069.
[27] Y. He, B. Yang, G. Cheng, Mater. Lett. 57 (2003) 1880–1884.
[28] A. Trovarelli, G. Dolcetti, C. De Leitenburg, J. Kaspar, P. Finetti, A.J. Santoni, Chem. Soc. Faraday Trans. 88 (1992) 1311–1319.
[29] S. Scirè, P.M. Riccobene, C. Crisafulli, Appl. Catal. B: Environ. 10 (2010) 109–117.